Modelling and experimental measurements of the mechanical response of piezoelectric structures from millimetre to micrometre

M. Bavencoffe, N. Tembhurnikar, B. Negulescu, J. Wolfman, G. Feuillard

Advances in Applied Ceramics: Structural, Functional and Bioceramics

Modelling and experimental measurements of the mechanical response of piezoelectric structures from millimeter to micrometer

--Manuscript Draft--

Manuscript Number:	AAC1951R1
Full Title:	Modelling and experimental measurements of the mechanical response of piezoelectric structures from millimeter to micrometer
Article Type:	Research paper
Keywords:	Piezoelectric material; Laser interferometry; Numerical modelling; Finite element method; Functional characterization; Impedancemetry
Corresponding Author:	Maxime Bavencoffe Institut National des Sciences Appliquees Centre Val de Loire FRANCE
Corresponding Author Secondary Information:	
Corresponding Author's Institution:	Institut National des Sciences Appliquees Centre Val de Loire
Corresponding Author's Secondary Institution:	
First Author:	Maxime Bavencoffe
First Author Secondary Information:	
Order of Authors:	Maxime Bavencoffe
	Nikhil Tembhurnikar
	Beatrice Negulescu
	Jerome Wolfman
	Guy Feuillard
Order of Authors Secondary Information:	
Abstract:	Laser interferometry techniques have shown their ability to assess the mechanical response of a piezoelectric thin film. To support these investigations, a numerical study based on the finite element method is carried out: three dimensional modellings of piezoelectric samples from bulk materials to thin films are examined. For each considered sample, a time dependent analysis and a frequency domain study are performed. By performing time dependent analysis, we obtain effective piezoelectric coefficient, d33, of the samples. Frequency domain study helps to calculate the frequency response of these samples. The calculated d33 values and the first frequency resonance values are then compared with the experimental data.

Modelling and experimental measurements of the mechanical response of piezoelectric structures from millimeter to micrometer

M. Bavencoffe[1*], N. Tembhurnikar[1], B. Negulescu[2], J. Wolfman[2], G. Feuillard[1]

[1]*GREMAN, UMR CNRS 7347, INSA Centre Val de Loire, 3 rue de la Chocolaterie, 41034 Blois, France*

[2]*GREMAN, UMR CNRS 7347, Université François-Rabelais, Faculté des Sciences et Techniques, Parc de Grandmont, 37200 Tours, France*

** Corresponding author: M. Bavencoffe, maxime.bavencoffe@insa-cvl.fr*

Modelling of the mechanical response of piezoelectric structures from millimeter to micrometer

Laser interferometry techniques have shown their ability to assess the mechanical response of a piezoelectric thin film. To support these investigations, a numerical study based on the finite element method is carried out: three dimensional modellings of piezoelectric samples from bulk materials to thin films are examined. For each considered sample, a time dependent analysis and a frequency domain study are performed. By performing time dependent analysis, we obtain effective piezoelectric coefficient, d33, of the samples. Frequency domain study helps to calculate the frequency response of these samples. The calculated d33 values and the first frequency resonance values are then compared with the experimental data.

Keywords: Piezoelectric material; Laser interferometry; Numerical modelling; Finite element method; Functional characterization; Impedancemetry

Introduction

Nowadays, piezoelectric materials have many applications in the fields of industry, medicine and research. Thin piezoelectric materials are important for developing MEMS devices [1], [2] such as autonomous wireless sensor network [3] and implanted medical devices [4]. Thereby, the research in the field of piezoelectric materials and in that new micro-electromechanical devices are getting much more inter-related. In this context, integrated structures based on the piezoelectric thin films are widely investigated and their characterisations become a crucial issue in the development of new applications. In the case of bulk material, resonance or out of resonance methods can be used to assess the material properties. The conventional static characterisation methods use the direct piezoelectric effect [5]. A static stress on the material generates a charge quantity on both faces of the material, which is measured, and the piezoelectric coefficient is determined. When applied to thin films, the method requires nano-positioning system to apply a uniform normal external stress on the sample. If not, the

consequence can be a bending of the structure leading to an incorrect measurement and a possible fracture of the sample. Inverse piezoelectric effect can also be used. In this case one has to measure the mechanical displacement for a given voltage. Today laser based interferometer has sensitivity less than 1 nm/V endowing displacement measurements on thin films possible [6]–[8].

This work addresses the development of a three dimensional (3D) modelling tool based on the finite element method (FEM) to support a laser based technique to characterize the mechanical response of piezoelectric samples in a quasistatic regime [9]. Different piezoelectric samples are here studied from millimeter size to micrometer size. Firstly, theoretical considerations on the determination of the effective piezoelectric coefficient, $\boldsymbol{d_{33}}$, of the active electro-material are briefly reported. Then, the different experimental setups used for the calculation of the frequency measurement and the effective piezoelectric coefficient measurement are presented. Finally, 3D FEM models are implemented for each investigated sample which enable the comparison of numerical to experimental results.

1 Theoretical considerations

The piezoelectric constitutive equations [10], [11] are defined as follows:

$$\boldsymbol{S_\alpha} = \boldsymbol{s^E_{\alpha\beta}} \boldsymbol{T_\beta} + \boldsymbol{d_{i\alpha}} \boldsymbol{E_i} \qquad (1)$$

$$\boldsymbol{D_i} = \boldsymbol{d_{i\alpha}} \boldsymbol{T_\alpha} + \boldsymbol{\varepsilon^T_{ij}} \boldsymbol{E_j} \qquad (2)$$

$$\alpha, \beta = 1, \cdots, 6 \qquad i, j = 1,2,3$$

These equations relate the mechanical strain and electrical displacement (respectively $\boldsymbol{S_\alpha}$ and $\boldsymbol{D_i}$) to the stress and electrical field (respectively $\boldsymbol{T_\beta}$ and $\boldsymbol{E_j}$) where $\boldsymbol{s^E_{\alpha\beta}}$ is the compliance tensor at constant electric field, $\boldsymbol{d_{i\alpha}}$ is the piezoelectric tensor and $\boldsymbol{\varepsilon^T_{ij}}$ the

permittivity tensor at constant stress. Figure 1 shows the orientation of the ceramic defined by α, β, i and j.

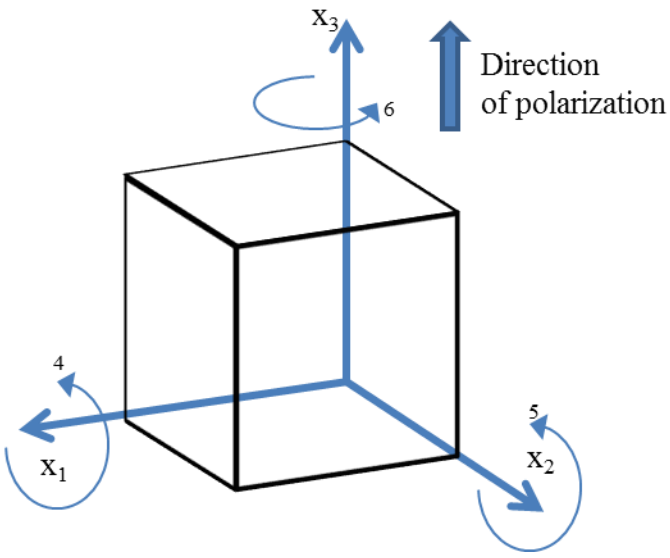

Figure 1 Notation of crystal axes with polarization direction

Equations (3), (4) and (5) are obtained from expanding the tensor notation.

$$\boldsymbol{S_1 = s_{11}^E T_1 + s_{12}^E T_2 + s_{13}^E T_3 + d_{31} E_3} \qquad (3)$$

$$\boldsymbol{S_3 = s_{13}^E (T_1 + T_2) + s_{33}^E T_3 + d_{33} E_3} \qquad (4)$$

$$\boldsymbol{D_3 = \varepsilon_3^T E_3 + d_{31}(T_1 + T_3) + d_{33} T_3} \qquad (5)$$

We consider a piezoelectric thin film deposited on an isotropic substrate and poled along the $\boldsymbol{x_3}$ direction. Then it is necessary to consider the clamping effects induced by other adjacent materials on the thin film. We assume that the displacement in axes 1 and 2 is negligible ($\boldsymbol{S_1 = S_2 = 0}$) and that the substrate is the dominant element ($\boldsymbol{T_1 = T_2 = T}$). With no applied stress, $\boldsymbol{T_3 = 0}$, we get

$$\boldsymbol{d_{33}^{eff} = d_{33} - 2 d_{31} \frac{s_{13}^E}{(s_{11}^E + s_{12}^E)}} \qquad (6)$$

Then, equation (6) gives the value of the effective electro-mechanical coefficient $\mathbf{d_{33}}$.

As referred from the analysis made by K. Lefki and G.J.M Dormans [5], this value is equal to the ratio of the elongation $\boldsymbol{\Delta l}$ of the sample in axis 3 to the applied voltage $\boldsymbol{V}$.

By inverse effect, when exposed to an AC electric field, a piezoelectric ceramic element changes dimensions cyclically at the cycling frequency of the field. This electric field produces a vibration whose amplitude corresponds to the displacement of the sample. Hence, with the help of equation (1) and for excitation frequencies much lower than the first cutoff frequency of the device, we can obtain $\boldsymbol{d_{33}^{eff}}$ as

$$\boldsymbol{d_{33}^{eff} = \frac{\Delta l}{V} = \frac{v}{U_{in} \times 2 \times \pi \times f_{in}}} \qquad (7)$$

where $\boldsymbol{v}$ is the normal velocity vibration of the piezoelectric sample, and $\boldsymbol{U_{in}}$ and $\boldsymbol{f_{in}}$ respectively the amplitude and the frequency of the sinusoidal input signal.

2 Experimental approach

The frequency at which the ceramic element vibrates most readily, and converts the electrical energy input into mechanical energy most efficiently, is the resonance frequency. At this particular frequency the admittance in an electrical circuit describing the sample is maximum. A Bode 100 Omicron impedance analyser is used to determine the frequency response of each investigated element (Figure 2).

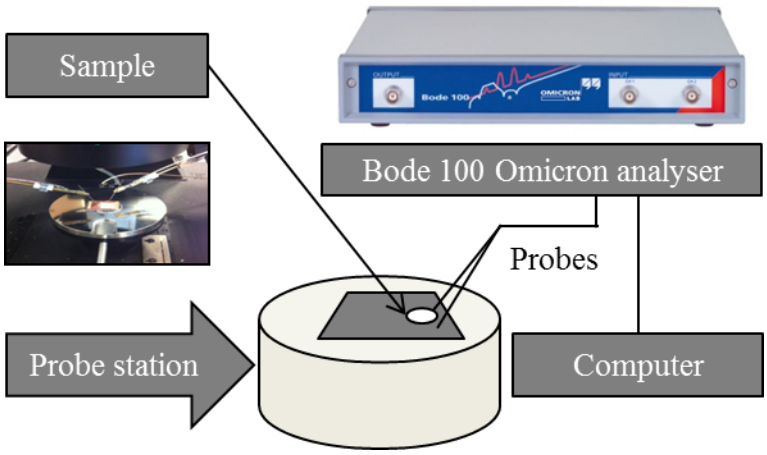

Figure 2 Bode 100 Omicron analyser setup

Then, the mechanical response of a sample in a quasistatic regime is obtained by measuring the displacement of its top surface by a laser setup (Figure 3) in a frequency range below the first resonance. The sample is placed on a probe station, connected to

an Agilent 33250A function generator and illuminated through a binocular microscope by a Polytec laser interferometer connected to its scanning system and controller. The laser set up allows displacement measurements of 50 nm/V or velocity measurements of 5mm/s/V. The demodulated laser signals and the excitation signals can be simultaneously visualized on a Lecroy 6050A oscilloscope.

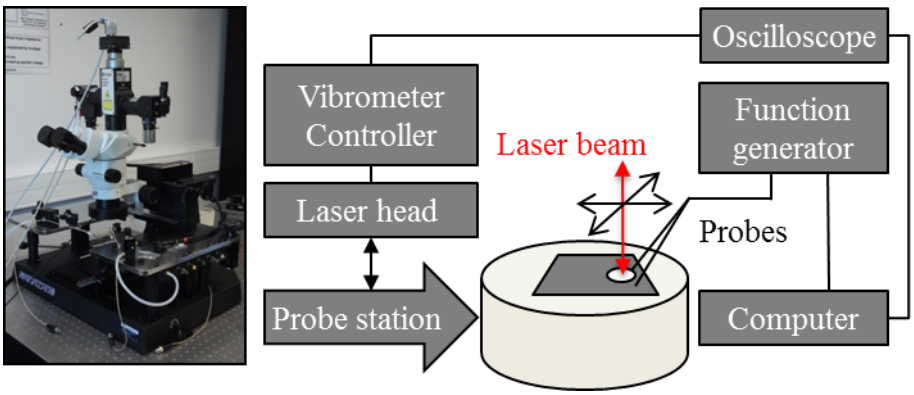

Figure 3 Laser setup

The whole experimental setup is controlled by a computer thanks to a Labview program which generates the input signals, acquires the output signals and performs the post-processing in Matlab. This post-treatment uses equation (7) to give the mean value of the calculated $\boldsymbol{d_{33}^{eff}}$ in pm/V for $\boldsymbol{N}$ demanded measurements (typically $\boldsymbol{N}$=10).

Measurements are carried out on four different samples presented in Figure 4: a PZ27 ceramic rod, dimensions 2x2x15mm; a PZ27 ceramic disc, 20mm diameter and 2mm thick; a $LiNbO_3$Y+36 single crystal, 12mm diameter and 0,5mm thick; a PZT thin film. This thin film consists of 240 nm $PbZr_{0.52}Ti_{0.48}O_3$ film deposited by sol-gel method obtained from STMicroelectronics (Tours, France) [12] [13] and Pt electrodes deposited by PVD (Physical Vapor Deposition) sputtering. Circular structures with diameters varying from 50µm to 1600µm were fabricated by conventional optical lithography and ion beam etching method. To allow the numerical study on an experimentally exploitable sample size, only the 400µm capacitors were considered.

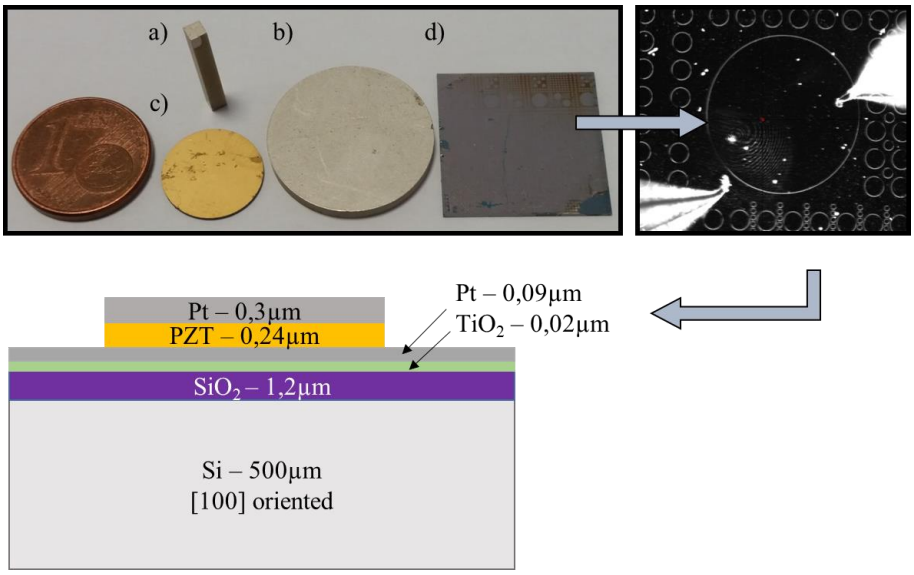

Figure 4 Investigated samples: a) PZ27 rod b) PZ27 disc c) $LiNbO_3$Y+36 single crystal d) PZT thin film

The Lithium Niobate sample, supplied by Roditi International Corporation Ltd., is used as reference sample as its properties are well investigated and reported in the literature data [14], [15]. The frequency response of this sample is presented in Figure 5. Its first occurring resonance (f_{r1}) is measured at 324,2kHz.

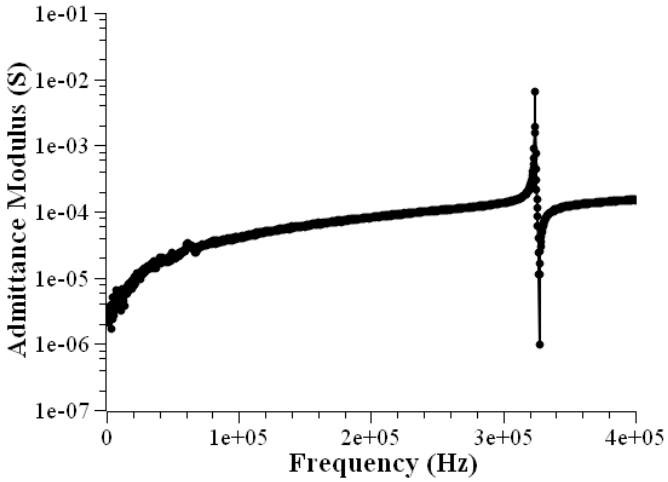

Figure 5 Frequency response of the $LiNbO_3$Y+36 single crystal

For each sample, Table 1 presents the value of the frequency of the first occurring resonance (f_{r1}) in kHz and of the d_{33}^{eff} in pm/V at 10kHz.

Table 1 Experimental measurements

SAMPLE	f_{r1} (kHz)	d_{33}^{eff} (pm/V) @ 10kHz
PZ27 rod	92,8	402,1
PZ27 disc	114,9	6,9
$LiNbO_3Y$+36 single crystal	324,2	34,8
PZT thin film	8884	99,1

Both of the PZ27 ceramic samples were manufactured by Meggitt-Ferroperm. Concerning the rod, the nominal value of its d_{33} given by the manufacturer is 425pm/V. We therefore have a discrepancy of 5,39% which can be explained by the variability of the ceramic properties from a batch to another.

3 Numerical modelling

To complete our experimental approach, a numerical study based on the finite element method is carried out with COMSOL Multiphysics® FEA software with the Structural Mechanics and the AC/DC modules.

COMSOL software has a special section of Material Library (based on the "Material Property Database (MPDB)," JAHM Software, Inc.) where numerous materials are available with their standard properties as Lithium Niobate. For PZ27, the properties have been taken from the Meggitt-Ferroperm's material data based on typical values. In the particular case of the thin film, the modelling of the 400µm capacitor has been lightened to the single piezoelectric layer considered made of PZ27. It has been done to limit the mesh size, to help the convergence and to stay in reasonable calculation times.

For each considered sample, a frequency domain analysis is firstly performed in a given frequency range to determine the quasistatic regime of the sample. A 3D modelling of the sample with free mechanical boundary conditions at its ends is built. The bottom surface in the model is grounded and an AC voltage source of amplitude 1V is applied on the top surface at the current frequency. The intensity is calculated at the terminals

of the sample and finally the electrical admittance is deduced for each studied frequency by application of the generalized Ohm's law. For each sample, Table 2 gives information on the mesh.

Table 2 Mesh information

SAMPLE	*type*	*number of elements*	*number of points*
PZ27 rod	quadrangular	475	720
PZ27 disc	triangular	696	585
$LiNbO_3$Y+36 single crystal	triangular	348	390
PZT thin film	triangular	214	248

Secondly, a time dependant analysis is done to obtain the normal displacement on the top surface of the sample: the bottom surface of the model is grounded and a sinusoidal electric potential (with parameters equivalent to the experimental excitation signal) is applied at its top surface. In the particular case of the thin film, the substrate clamping is taken into account by a fixed constraint mechanical boundary condition at the bottom surface of the piezoelectric layer. With the help of the displacement values obtained at the top surface of the sample, the piezoelectric coefficient (d_{33}) is calculated from equation (7).

From the simulations, we then obtain the value of the frequency of the first occurring resonance in kHz and of the d_{33}^{eff} in pm/V. For each sample, these results are reported in Table 3.

Table 3 Numerical results

SAMPLE	f_{r1} (kHz)	d_{33}^{eff} (pm/V) @ 10kHz
PZ27 rod	98,4	423
PZ27 disc	125,3	7,4
$LiNbO_3$Y+36 single crystal	321,5	36,3

PZT thin film	7960	116

Concerning the rod, we notice a discrepancy of 0,47% with the nominal value of its d_{33} given by the manufacturer.

Figure 6 presents the frequency response of the LiNbO3Y+36 single crystal obtained by numerical modelling compared to its experimental curve. Compared to the experiment, there is a difference of less than 1% in frequency. The amplitude mismatching between the two curves could be reduced by a better appreciation of the actual tensors of the material [16].

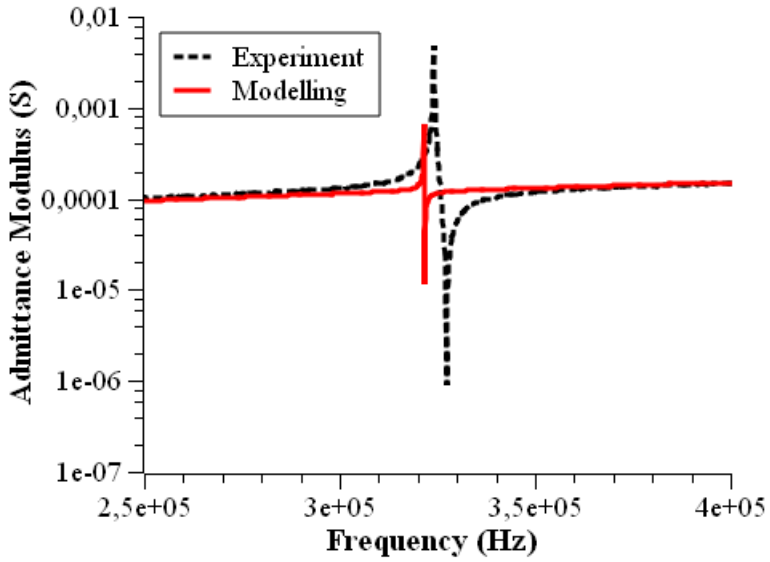

Figure 6 Frequency response of the $LiNbO_3Y+36$ single crystal: experiment vs. modelling

4 Discussion

Table 4 presents for each sample the percentage of difference between experimental and modelling results.

Table 4 Experiment vs. modelling

SAMPLE	f_{r1} (kHz)	d_{33}^{eff} (pm/V)
	Δ (%)	Δ (%)

PZ27 rod	6	4,9
PZ27 disc	9	5,9
$LiNbO_3Y+36$ single crystal	0,83	4,1
PZT thin film	10,4	14,5

Finally, the discrepancy between modelling and experiment is less than 15%. This discrepancy increases as the size of piezoelectric film decreases from millimeter to micrometer. In case of thick films, the whole geometry is reduced to a piezoelectric layer, whereas for thin films, many layers such as platinum electrodes, titanium dioxide, silicon dioxide and silicium wafer are present.

Thus, number of parameters such as contribution of additional layers or substrate clamping are not well taken into account. Indeed, for these samples the measured d_{33}^{eff} parameter is related to the bulk d_{33} parameter by equation (6) depending on the unclamped mechanical compliances of the piezoelectric film and on the unclamped transverse piezoelectric coefficient. Likewise, the substrate bending during measurement can also influence the measurements [17] [18] especially when done on large diameter electrodes.

In addition, bulk material data were taken for calculation while it is well known that in the case of thin film the different material tensors are very often modified due to microstructural differences (mostly in grain size) and to enhanced interfacial effects generated by the reduced dimensionality [19] [20].

Furthermore, the accuracy in the results can be limited by the precise knowledge of the elastic, dielectric and piezoelectric properties of the piezoelectric material too. The characterization step is mainly performed by experiments on test samples using the IEEE standard method [21]. Usually, the manufacturer conducts this characterization step, offering a unique database, with the error measurements, regardless of the shape or a specific batch of each kind of piezoelectric ceramic or single crystal [22]. Even if these values are determined with a relatively good accuracy (often a maximum of ±10%), a significant difference can appear between the simulations and the actual behavior for a piezoelectric sample. One rising approach to determine the properties of piezoelectric materials are the FEM-based methods . Most of them adjust the theoretical electrical impedance curve to fit with the experimental one: an automatic algorithm is implemented to find the material properties that minimize the difference between the

numerical impedance curve and the experimental one, in a given frequency range [16], [23]–[28].

At last, the samples have ben modelled in mechanical free boundary conditions even if they are in reality laid down on a platinum and that tungsten tips are used to resumption of electrical contact.

Conclusion

The ability to predict the mechanical response of piezoelectric samples from finite element modelling has been demonstrated and compared to experimental data. The first resonance values and the d_{33} values obtained from this first modelling step are in a good agreement with the experimental ones for the milimetric sized samples. 10 to 15 % differences between these values are obtained in the micrometric sized sample indicating that other effects such as substrate clamping and contribution of additional layers should be better taken into account both experimentally and numerically. The consideration of these effects will be the subject of a future work.

Acknowledgment

This work is funded by Région Centre-Val de Loire in the frame of the project "COMHET". We would like to thank STMicroelectronics (Tours, France) for providing with the thin film samples.

References

1. Trolier-Mckinstry S, Muralt P. Thin film piezoelectrics for MEMS. J Electroceramics. 2004;12(1-2):7-17.
2. Smith GL, Pulskamp JS, Sanchez LM, et al. PZT-Based Piezoelectric MEMS Technology. Green DJ, ed. J Am Ceram Soc. 2012;95(6):1777-1792.
3. Anton SR, Sodano H a. A review of power harvesting using piezoelectric materials (2003–2006). Smart Mater Struct. 2007;16(3):R1-R21.

4. Lewandowski BE, Kilgore KL, Gustafson KJ. Feasibility of an Implantable, Stimulated Muscle-Powered Piezoelectric Generator as a Power Source for Implanted Medical Devices. In: Energy Harvesting Technologies. Boston, MA: Springer US; 2009:389-404.

5. Lefki K, Dormans GJM. Measurement of Piezoelectric Coefficients of Ferroelectric Thin Films. J Appl Phys. 1994;76(3):1764-1767.

6. Ledermann N, Muralt P, Baborowski J, et al. {1 0 0}-textured, piezoelectric Pb(Zrx, Ti1-x)O3 thin films for MEMS: Integration, deposition and properties. Sensors Actuators, A Phys. 2003;105(2):162-170.

7. Pérez de la Cruz J, Joanni E, Vilarinho PM, et al. Thickness effect on the dielectric, ferroelectric, and piezoelectric properties of ferroelectric lead zirconate titanate thin films. J Appl Phys. 2010;108(11):114106.

8. Yao K, Tay FEH. Measurement of longitudinal piezoelectric coefficient of thin films by a laser-scanning vibrometer. IEEE Trans Ultrason Ferr Freq Control. 2003;50(2):113-116.

9. Feuillard G, Bavencoffe M, Fortineau J, et al. Measurement of the effective piezoelectric coefficient on PZT fim integrated structures using laser interferometry. In: Electroceramics for End-Users VII Conference. Les Arcs (France); 2013.

10. Jordan TL, Ounaies Z. Piezoelectric Ceramics Characterization. Hampton, Virginia; 2001.

11. Torah RN, Beeby SP, White NM. Experimental investigation into the effect of substrate clamping on the piezoelectric behaviour of thick-film PZT elements. J Phys D Appl Phys. 2004;37:1074-1078.

12. Chentir MT, Bouyssou E, Ventura L, et al. Leakage current evolution versus

dielectric thickness in lead zirconate titanate thin film capacitors. J Appl Phys. 2009;105(6).

13. Chentir MT, Ventura L, Bouyssou E, et al. Cavity origin and influence on reliability in lead zirconate titanate thin film capacitors. J Appl Phys. 2009;106(5):1-6.

14. Warner AW, Onoe M, Coquin GA. Determination of Elastic and Piezoelectric Constants for Crystals in Class (3 *m*). J Acoust Soc Am. 1967;42(6):1223-1231.

15. Ogi H, Kawasaki Y, Hirao M, et al. Acoustic spectroscopy of lithium niobate: Elastic and piezoelectric coefficients. J Appl Phys. 2002;92(5):2451-2456.

16. Hoang T, Ferin G, Rosinski B, et al. Characterization of a thin piezoelectric material before integration into a cantilever-based mechanical energy harvester. In: IEEE International Ultrasonics Symposium, IUS. Vol 2016-Novem. IEEE; 2016:1-4.

17. Herdier R, Jenkins D, Dogheche E, et al. Laser Doppler vibrometry for evaluating the piezoelectric coefficient d33 on thin film. Rev Sci Instrum. 2006;77(9).

18. Leighton GJT, Huang Z. Accurate measurement of the piezoelectric coefficient of thin films by eliminating the substrate bending effect using spatial scanning laser vibrometry. Smart Mater Struct. 2010;19(6):65011.

19. Shaw TM, Trolier-McKinstry S, McIntyre PC. The properties of Ferroelectric Films at Small Dimensions. Annu Rev Mater Sci. 2000;30(1):263-298.

20. Wasa K, Kanno I, Kotera H. Fundamentals of thin film piezoelectric materials and processing design for a better energy harvesting MEMS. Power MEMS 2009. 2009;61(January):61-66.

21. The Institute of Electrical and Electronics Engineers Inc. IEEE Standard on

Piezoelectricity. 1988:84.

22. Meggitt A/S Ferroperm. Tolerances and Resources. https://www.meggittferroperm.com/resources/tolerances/.

23. Joo H-W, Lee C-H, Jung H-K. Identification of the piezoelectric material coefficients using the finite element method with an asymptotic waveform evaluation. Ultrasonics. 2004;43(1):13-19.

24. Lahrner T, Kaltenbacher M, Kaltenbacher B, et al. FEM-Based determination of real and complex elastic, dielectric, and piezoelectric moduli in piezoceramic materials. IEEE Trans Ultrason Ferroelectr Freq Control. 2008;55(2):465-475.

25. Jonsson UG, Andersson BM, Lindahl OA. A FEM-based method using harmonic overtones to determine the effective elastic, dielectric, and piezoelectric parameters of freely vibrating thick piezoelectric disks. IEEE Trans Ultrason Ferroelectr Freq Control. 2013;60(1).

26. Pérez N, Carbonari RC, Andrade MAB, et al. A FEM-based method to determine the complex material properties of piezoelectric disks. Ultrasonics. 2014;54(6):1631-1641.

27. Rupitsch SJ, Ilg J. Complete characterization of piezoceramic materials by means of two block-shaped test samples. IEEE Trans Ultrason Ferroelectr Freq Control. 2015;62(7):1403-1413.

28. Rouffaud R, Hladky-Hennion A-C, Levassort F. A combined genetic algorithm and finite element method for the determination of a practical elasto-electric set for 1-3 piezocomposite phases. Ultrasonics. 2017;77:214-223.

List of figure captions

Figure 1 Notation of crystal axes with polarization direction

Figure 2 Bode 100 Omicron analyser setup

Figure 3 Laser setup

Figure 4 Investigated samples: a) PZ27 rod b) PZ27 disc c) $LiNbO_3Y+36$ single crystal d) PZT thin film

Figure 5 Frequency response of the $LiNbO_3Y+36$ single crystal

Figure 6 Frequency response of the $LiNbO_3Y+36$ single crystal: experiment vs. modelling

Colour figure (online only)

Click here to download Colour figure (online only) figure1.tif

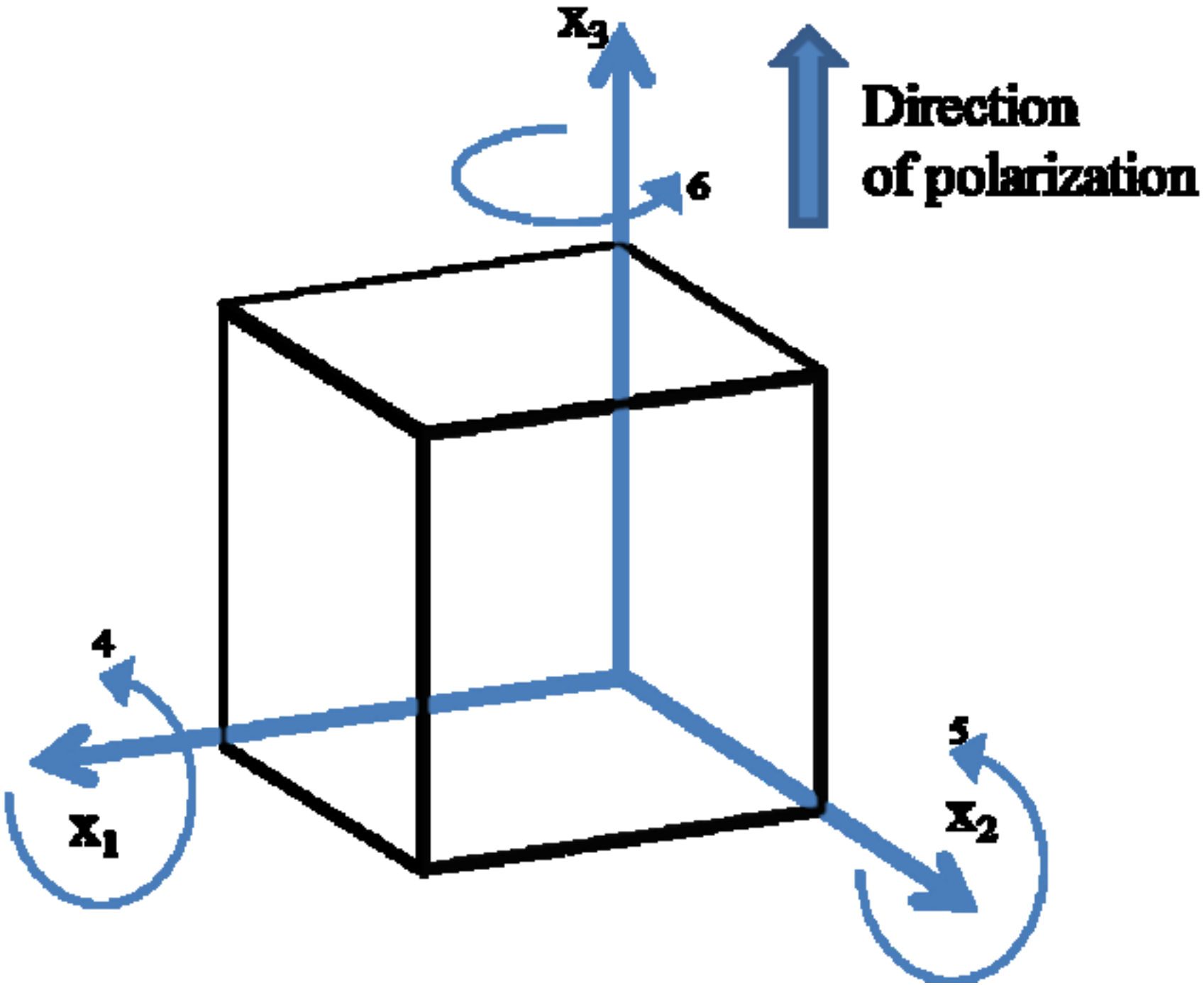

Colour figure (online only)

Click here to download Colour figure (online only) figure2.tif

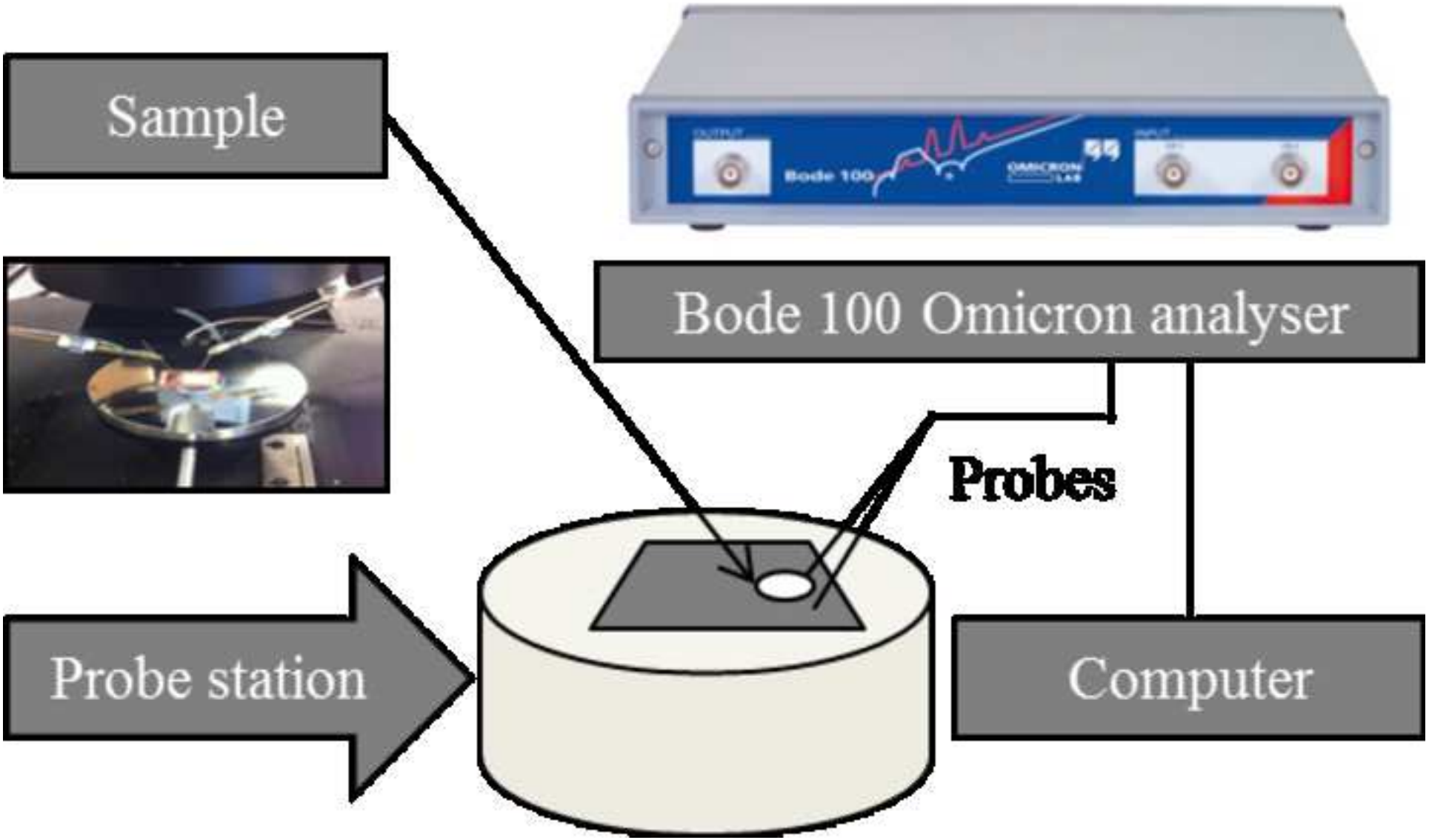

Colour figure (online only)

Click here to download Colour figure (online only) figure3.tif

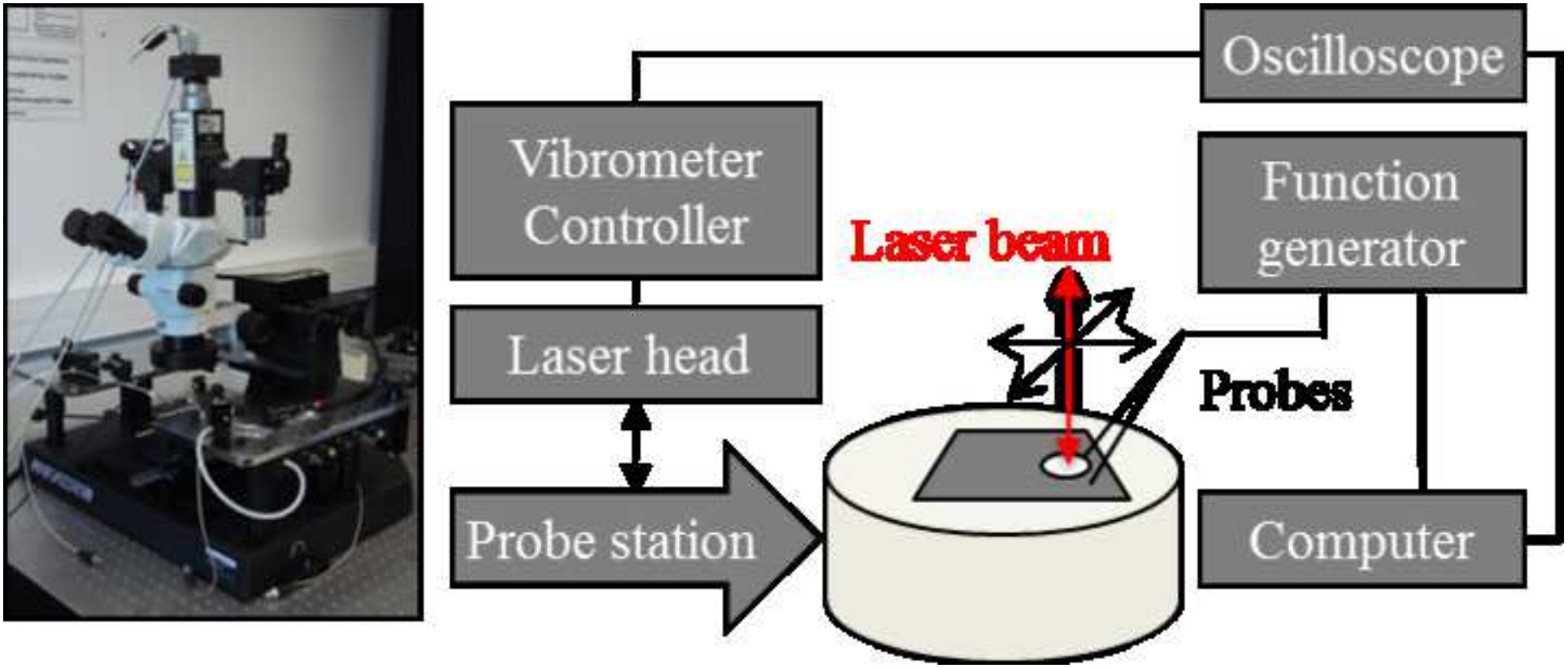

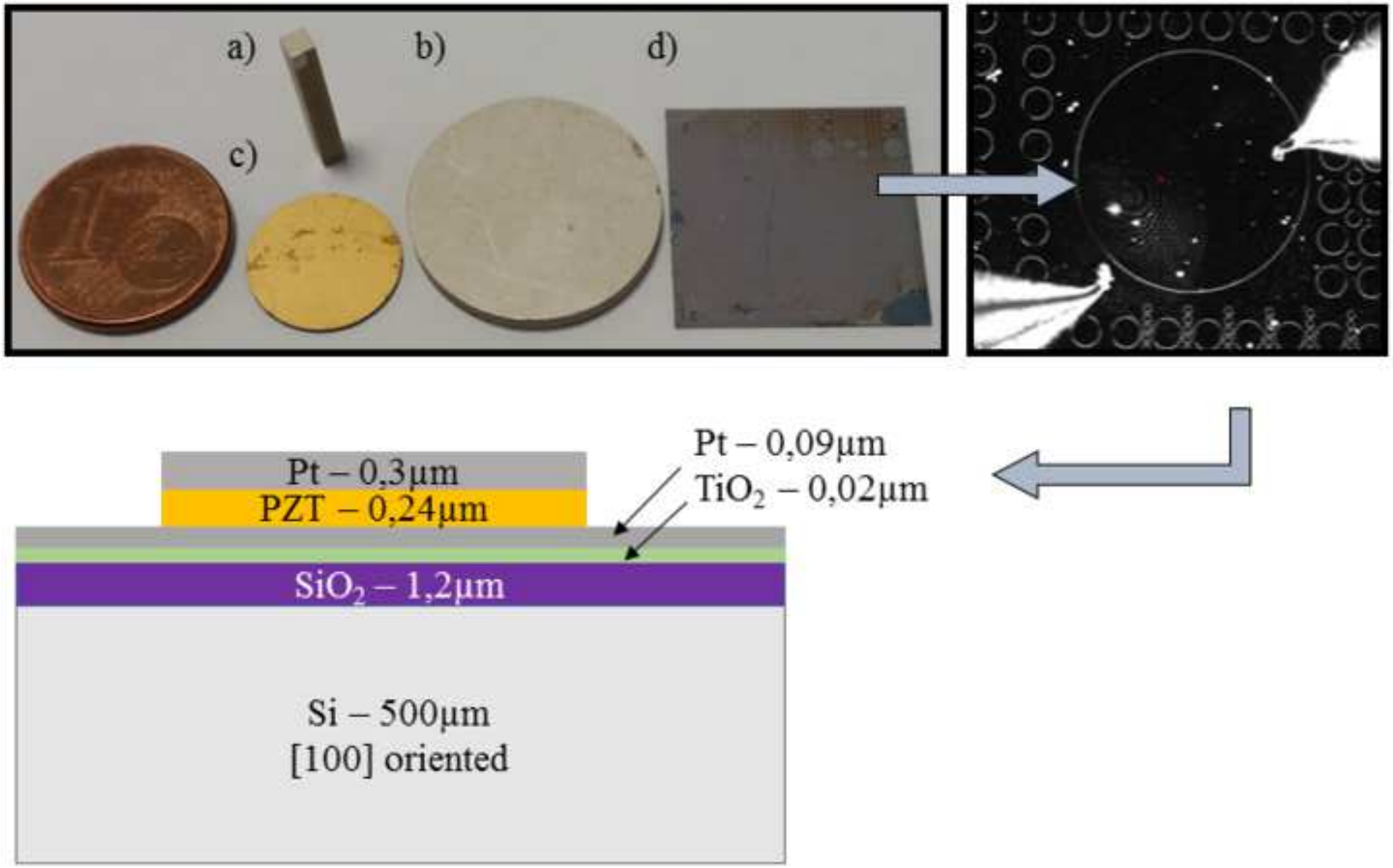

Non-colour figure

Click here to download Non-colour figure figure5.tiff

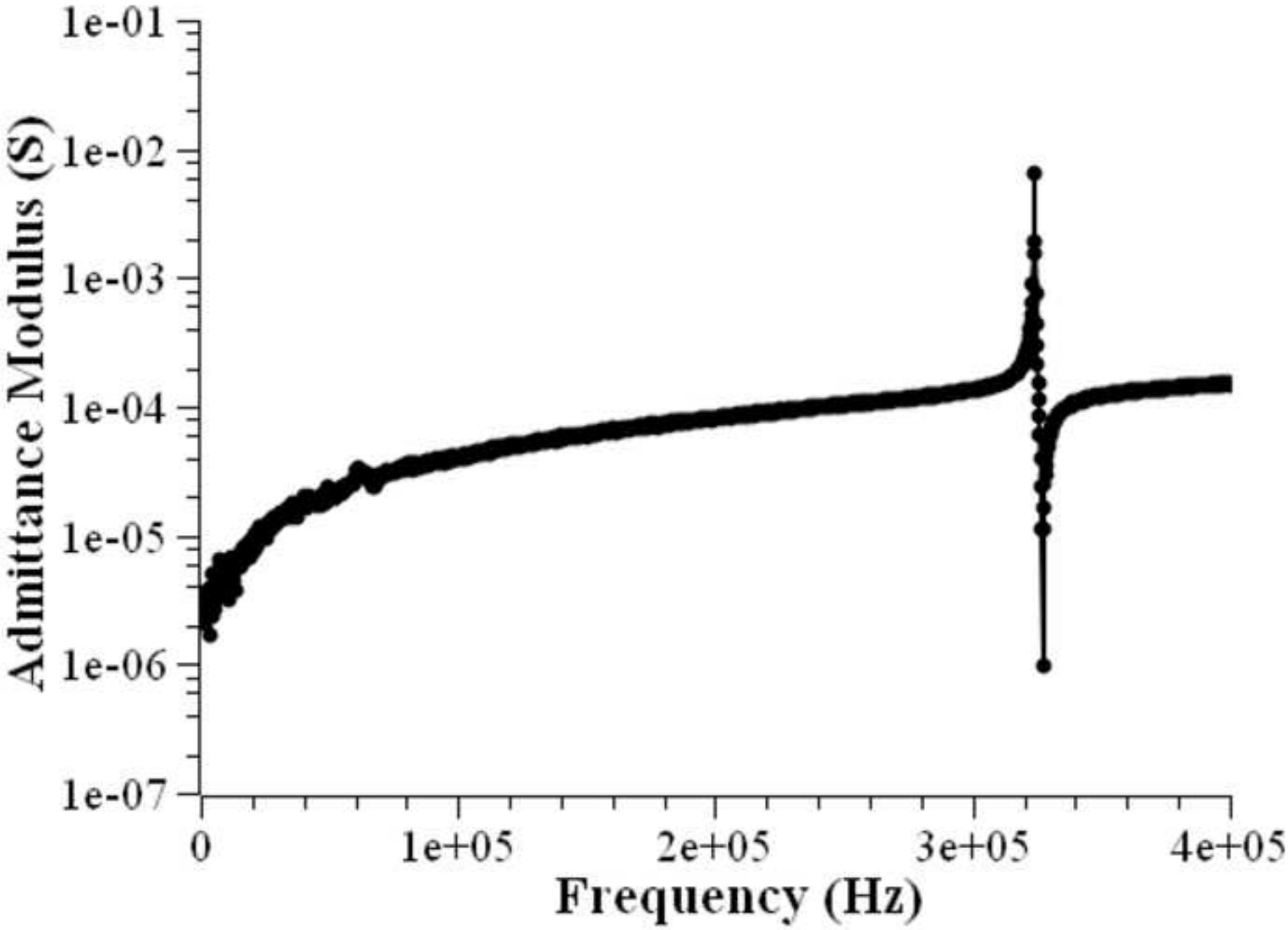

Colour figure (online only)

Click here to download Colour figure (online only) figure6.tiff